

Role of $\alpha 2\delta 3$ in Cellular Synchronization of the Suprachiasmatic Nucleus Under Constant Light Conditions

Masahiro Matsuo,^{a,b†} Kazuyuki Seo,^{a†} Naoki Mizuguchi,^a Fumiyoshi Yamazaki,^a Shoichi Urabe,^a Naoto Yamada,^b Masao Doi,^a Keiko Tominaga^c and Hitoshi Okamura^{a,d*}

^a Graduate School of Pharmaceutical Sciences, Kyoto University, Kyoto 606-8501, Japan

^b Department of Psychiatry, Shiga University of Medical Science, Shiga 520-2192, Japan

^c Graduate School of Frontier Biosciences, Osaka University, Suita Osaka 565-0871, Japan

^d Department of Neuroscience, Graduate School of Medicine, Kyoto University, Kyoto 606-8501, Japan

Abstract—By the effort to identify candidate signaling molecules important for the formation of robust circadian rhythms in the suprachiasmatic nucleus (SCN), the mammalian circadian center, here we characterize the role of $\alpha 2\delta$ proteins, synaptic molecules initially identified as an auxiliary subunit of the voltage dependent calcium channel, in circadian rhythm formation. *In situ* hybridization study demonstrated that type 3 $\alpha 2\delta$ gene ($\alpha 2\delta 3$) was strongly expressed in the SCN. Mice without this isoform ($Cacna2d3^{-/-}$) did not maintain proper circadian locomotor activity rhythms under a constant light (LL) condition, whereas under a constant dark (DD) condition, these mice showed a similar period length and similar light-responsiveness as compared to wild type mice. Reflecting this behavioral phenotype, $Cacna2d3^{-/-}$ mice showed a severely impaired *Per1* expression rhythm in the SCN under LL, but not under DD. Cultured SCN slices from *Per1-luc* transgenic $Cacna2d3^{-/-}$ mice revealed reduced synchrony of *Per1-luc* gene expression rhythms among SCN neurons. These findings suggest that $\alpha 2\delta 3$ is essential for synchronized cellular oscillations in the SCN and thereby contributes to enhancing the sustainability of circadian rhythms in behavior. © 2021 The Author(s). Published by Elsevier Ltd on behalf of IBRO. This is an open access article under the CC BY-NC-ND license (<http://creativecommons.org/licenses/by-nc-nd/4.0/>).

Key words: circadian rhythms, suprachiasmatic nucleus, alpha2delta3, light.

INTRODUCTION

In mammals, internal time is orchestrated by the master clock in the hypothalamic suprachiasmatic nucleus (SCN), whose coherent output signal synchronizes cellular clocks throughout the body (Reppert and Weaver, 2002; Mohawk et al., 2012; Herzog et al., 2017). The previous observation of tetrodotoxin-induced arrhythmicity of clock genes expression in individual cells in the SCN, strongly indicates the importance of synaptic transmission on circadian rhythm generation (Yamaguchi et al., 2003). The involvement of neuronal activity in the oscillation of the circadian clock has also been suggested in *Drosophila* (Nitabach et al., 2002; Harrisingh and Nitabach, 2008). A number of neurotransmitters, receptors and their coupled intracellular signals are involved in the circadian generation and synchronization of cellular

clocks in the SCN (Herzog et al., 2017). To identify candidate signaling molecules that might contribute to SCN rhythm formation, we designed a screening strategy called SCN-Gene Project (Okamura, 2007; Doi et al., 2011) in which we (i) used histochemistry to identify genes whose expression is enriched in the mouse SCN, (ii) generated mutant mice lacking candidate genes of interest, and (iii) measured the locomotor activity at various environmental conditions.

In searching the substances involved in neuronal synaptic functions in the SCN, we focused on $\alpha 2\delta$ membrane-anchored extracellular glycoproteins ($\alpha 2\delta 1$, $\alpha 2\delta 2$, $\alpha 2\delta 3$, $\alpha 2\delta 4$) (Dooley et al., 2007; Hoppa et al., 2012; Campiglio and Flucher, 2015), since these proteins are mainly associated with synaptic terminals rather than cell bodies in brain neurons (Cole et al., 2005; Dooley et al., 2007; Hoppa et al., 2012). The $\alpha 2\delta$ proteins are traditionally considered to be auxiliary subunits of voltage-gated calcium channel that influence the channels' biophysical properties (Dolphin, 2012). Accumulating evidence indicates that $\alpha 2\delta$ subunits may also have roles in the nervous system that are not directly linked to calcium channel functions such as that in synaptogenesis. $\alpha 2\delta 2$ is reported to have synapse-forming ability in cere-

*Correspondence to: H. Okamura, Kyoto University, Graduate School of Medicine, Department of Neuroscience, Yoshida-Konoe-cho, Sakyo-ku, Kyoto 606-8501, Japan. Fax: +81-75-753-9265. E-mail address: okamura.hitoshi.4u@kyoto-u.ac.jp (H. Okamura).

[†] These authors equally contributed to this work.
Abbreviations: CT, circadian time; EDTA, ethylenediaminetetraacetic acid; rPSD, relative power spectral density; SCN, suprachiasmatic nucleus.

bellar climbing fiber synapses (Beeson et al., 2020) and in inner hair cell synapses (Fell et al., 2016). $\alpha 2\delta$ proteins are also molecular target of gabapentin and pregabalin (Field et al., 2006; Eroglu et al., 2009; Neely et al., 2010; Alles et al., 2020), widely used as antiepileptics, and are also used for neuropathic pain (Dworkin et al., 2007) or sensorimotor symptoms of restless-leg syndrome (Winkelman et al., 2016; Iftikhar et al., 2017) in humans.

Here we identify the abundant expression of subtype 3 of $\alpha 2\delta$ proteins (= $\alpha 2\delta 3$) in the SCN, and report its circadian oscillatory expression in the SCN. We also examined the circadian locomotor activity rhythms of mice lacking the $\alpha 2\delta 3$ gene (*Cacna2d3*-deficient mice), and found that they show markedly weakened rhythmicity. Particularly, when maintained under constant light illumination, *Cacna2d3*-deficient mice displayed arrhythmicity. It is noteworthy that coherent synchrony of the cellular clocks was impaired in the SCN of *Cacna2d3*-deficient mice *in vivo* (detected by daily changes of digoxigenin-*in situ* hybridization study of *Per* genes) and in *in vitro* organotypic slice culture, indicating that the ensemble made by thousands of clock neurons in the SCN is deteriorated in the absence of $\alpha 2\delta 3$.

EXPERIMENTAL PROCEDURES

Animals and behavioral analysis

Cacna2d3-knockout mice (*Cacna2d3*^{-/-}) that were generated by Deltagen (San Mateo, CA, USA) were obtained from Jackson Laboratory (Bar Harbor, USA). These mice developed normally in young ages. We also evaluated behaviors at 8–10 weeks of age, and did not find any prominent neurological impairment such as cerebellar ataxia, vestibular ataxia and chorea. Eight to twelve weeks old *Cacna2d3*^{-/-} mice and their littermate wildtype (WT) mice were individually housed under 12-h light: 12-h dark (LD) cycles at 22 °C ± 2 °C for at least one week before the experiments, and food and water were provided *ad libitum*. Locomotor activity was detected by infrared sensors (FA-05 F5B; Omron, Japan), and the data were analyzed with the Clocklab software (ActiMetrics; Wilmette, IL, USA).

The free running period was determined with a linear regression line fit to the activity onsets of 7 consecutive days in the continuous dark (DD) condition. For the phase-dependent phase-shift experiments, mice allocated in DD were individually exposed to a 30-min light pulse (200 lux fluorescent light) at three different time points: circadian time (CT) 6, 14, and 22. Phase shifts were quantified as the time difference between the regression lines of activity onset before and after the light pulse; the regression lines were depicted based on the 7-day activity onset before the light stimulation and 7-day activity onset 3 days after the light stimulation. For the quantification of rhythmicity, the relative power spectral density (rPSD) was calculated based on the function embedded in the ClockLab software. After filtering with a Blackman-Harris window, a Fast Fourier Transform was applied to the 7 days of locomotor

activity data. The strength of rhythmicity was given as the rPSD, which corresponds to the relative signal strength of frequency close to the circadian period (0.036–0.048 cycles/h) divided by the cumulative strength of all frequencies (0–1 cycles/h). All experiments were approved by the Animal Experimentation Committee of Kyoto University.

Preparing of tissues

For sampling in the LD or DD conditions, mice were sacrificed in the last LD cycle or in the second continuous dark cycle every 4 h starting at Zeitgeber time (ZT)0 or CT0; ZT12 was defined as the light onset time in LD, and CT12 was defined as the activity onset time in DD. For sampling in the continuous light (LL) condition, the CT of arrhythmic mice was determined by linear extrapolation of the regression line to the first 7 days activity onset (CT12) in LL. Mice were deeply anesthetized with ether and intracardially perfused with 10 mL of autoclaved ice-cold saline, followed by 20 mL of 4% paraformaldehyde in 0.1 M phosphate buffer (PB; pH 7.4). Animals housed in the dark were anesthetized under a safety dim red light. The brains were removed, fixed for 24 h at 4 °C, and placed in 0.1 M PB with 20% sucrose for 24 h. Brains were frozen using dry ice and stored at –80 °C until use. Coronal brain sections, 40 μ m in thickness, were prepared by cryostat (CM3050S, Leica, Germany).

In situ hybridization

Gene specific antisense probes were generated to cover the following regions: 2141–2683 bp of the *Cacna2d1* (NM_001110843.1), 1172–1643 bp of *Cacna2d2* (NM_001174047.1), 2443–2986 bp of *Cacna2d3* (NM_009785.1), 2458–2930 bp of *Cacna2d4* (NM_001033382.2), 812–1651 bp of *Per1* (NM_011065), 1435–1919 bp of *Per2* (NM_011066.3). The corresponding cDNA fragments were cloned and used as a template for antisense cRNA probes. Radiolabeled probes and digoxigenin-labeled probes were prepared using [³³P]UTP (PerkinElmer, Waltham, MA, USA) and digoxigenin-UTP (Roche Diagnostics) with a standard protocol for the cRNA synthesis, respectively.

Free-floating tissue sections were washed (4 × SSC), processed with proteinase K (1 μ g/mL, 0.1 M Tris buffer, 50 mM ethylenediaminetetraacetic acid (EDTA), pH 8.0, 15 min, 37 °C), and then acetylated (0.25% acetic anhydride, 0.1 M triethanolamine, 10 min). After washing (4 × SSC, 10 min), the sections were incubated with radiolabeled riboprobes (55% formamide, 10% dextran sulfate, 10 mM Tris-HCl, 1 mM EDTA, 0.6 M NaCl, 0.2% N-laurylsarcosine, 500 μ g/mL tRNA, 1 × Denhardt's, 0.25% sodium dodecyl sulfate, 10 mM dithiothreitol, pH 8.0, 16 h, 60 °C) (Shigeyoshi et al., 1997). After hybridization, the sections were rinsed twice (2 × SSC/50% formamide, 45 min and 15 min, 60 °C) and treated with RNase (10 μ g/mL, 10 mM Tris-HCl, 1 mM EDTA, 0.5 M NaCl, pH 8.0, 30 min, 37 °C). After sequential washes (2 × SSC/50% formamide, 15 min, 60 °C, then

0.4 × SSC, 30 min, 60 °C), the sections were mounted onto gelatin-coated microscope slides, and air-dried.

For digoxigenin-labeled *in situ* hybridization, 30 μm-thick coronal sections were used. After *in situ* hybridization, the sections were processed with a nucleic acid detection kit (Roche Diagnostics) following the manufacturer's protocol.

For quantification of gene transcription, radiolabeled sections were exposed to Biomax films (Kodak, Rochester, NY, USA) for 5 days together with ¹⁴C- autoradiographic micro scales (Amersham, UK). Autoradiography films were then quantified with the MCID image analyzing system (Imaging Research Inc., St. Catharines, Ontario, Canada). Ten sections of the SCN were then summed. Data were analyzed by one-way ANOVA, followed by Sheffe's multiple comparisons.

X-gal staining

For X-gal staining, the free-floating sections were washed twice (0.1 M PB, 2 mM MgCl₂, 5 mM EGTA, 5 min and 30 min), and permeabilized (0.1 M PB, 2 mM MgCl₂, 0.01% sodium deoxycholate, 0.02% Nonidet P40, 5 min, room temperature). The sections were then incubated in X-gal staining buffer (5 mM K-ferricyanide, 5 mM K-ferrocyanide, 1 mg/mL X-gal, 0.1 M PB, 2 mM MgCl₂, 0.01% sodium deoxycholate, 0.02% Nonidet P40, 3 h, room temperature) in light-proof containers. The stained sections were coverslipped with Entellan (Merk Chemicals) after dehydration.

Organotypic SCN slice culture

The transgenic mice carrying a firefly luciferase reporter gene fused with the upstream region of *mPer1* (*Per1-luc* transgenic mice) (Yamaguchi et al., 2000) were crossed with *Cacna2d3*^{-/-} mice to produce *Per1-luc-WT* or *Per1-luc-Cacna2d3*^{-/-} mice. The SCN slices of neonatal transgenic mice (4- to 7-days old) were prepared as described previously (Yamaguchi et al., 2003). Each of the SCN slices was maintained at 35 °C in a sealed 35-mm petri dish with 1 mL of the culture medium (50% minimum essential medium, 50% Hank's balanced salt solution, 36 mM glucose, 25 units/mL penicillin, and 25 mg/mL streptomycin) containing 1 mM D-luciferin during bioluminescence recording. We measured SCN luminescence after culturing for 7 days. The luminescence from the cultured SCN was measured every 20 min with a highly sensitive cryogenic CCD camera (Pixel Vision) equipped with a microscope (Carl Zeiss). Observed image data were filtered through a median filter to eliminate cosmic-ray-induced background noise.

RESULTS

α2δ3 is strongly expressed in the SCN neurons

α2δ proteins exist in multiple isoforms in humans and mice: there are four different isoforms (*Cana2d1*, *Cacna2d2*, *Cana2d3*, and *Cacna2d4*), each showing different tissue specificity (Dolphin, 2012). To identify which isoform(s) is expressed in the SCN, we performed *in situ* hybridization using radiolabeled gene-specific

probes. The SCN was sampled at ZT4 and ZT16, which correspond to time of day and night, respectively. We observed that the gene encoding α2δ3 (*Cacna2d3*) displayed robust expression in the SCN at ZT4, compared to ZT16, while the expressions of other isoforms (*Cana2d1*, *Cacna2d2*, and *Cacna2d4*) were low at both timepoints (Fig. 1A). These observations led us to focus on *Cacna2d3*.

To characterize the daily expression profiles of *Cacna2d3*, we quantified *Cacna2d3* expression levels at six timepoints throughout a day under a regular 12-h light:12-h dark (LD) cycle condition as well as under constant darkness (DD). In LD, *Cacna2d3* displayed peak expression at ZT0 and gradually decreased to approximately 75% at ZT12 (Fig. 1B, upper panel) (ZT0 vs ZT12; ***p* < 0.01 one-way ANOVA, followed by Sheffe's multiple comparisons). Because a similar fluctuation was observed in DD (Fig. 1B, lower panel) (CT0 vs CT12; ***p* < 0.01 one-way ANOVA, followed by Sheffe's multiple comparisons), it is plausible that this mild oscillation of *Cacna2d3* expression in the SCN is under the control of the endogenous clock.

A topographical distribution of *Cacna2d3* in the SCN was further investigated by *in situ* hybridization with digoxigenin-labeled probe at ZT4 and ZT16. It was found that the distribution of *Cacna2d3* expression is confined to the ventral part of the SCN at both timepoints (Fig. 1C).

Circadian period and phase response to light are not altered in *Cacna2d3*^{-/-} mice

The above histological surveys showed that α2δ3 is the dominant α2δ subunit in the SCN. To identify the role of α2δ3 in the circadian rhythm *in vivo*, we used mice with a targeted deletion of *Cacna2d3* (*Cacna2d3*^{-/-}). In *Cacna2d3*^{-/-} mice, the coding sequence of *Cacna2d3* was replaced with a β-gal cassette, which led to robust β-gal expression in the SCN with the higher expression in its ventral subdivision (Fig. 2A). Compared to WT mice, *Cacna2d3*^{-/-} mice showed no obvious difference in size or weight of body, in agreement with a report by Deltagen (<http://www.informatics.jax.org/allele/MGI:3604520>).

Cacna2d3^{-/-} mice were tested for circadian activity rhythms. These mice showed normal entrainment to the LD conditions (Fig. 2B). In the DD condition, the period length of the endogenous circadian clock was not affected by the deletion of *Cacna2d3* (*Cacna2d3*^{+/+} vs *Cacna2d3*^{-/-}: 23.83 ± 0.01 h vs 23.69 ± 0.01 h; *p* > 0.1, *n* = 8, Student's *t*-test) (Fig. 2B, C). Since *Cacna2d3* expression was localized in the ventrolateral region of the SCN, where a light input signal from the retina triggers expression of light-responsive clock genes, we examined whether light influence is altered or not in *Cacna2d3*^{-/-} mice. We examined the magnitude of phase-response to light stimulation at three different timepoints, CT6, CT14, and CT22; light pulse administered at subjective day (CT6), subjective evening (CT14), or late subjective night (CT22) causes no phase shift, phase delay, or phase advance of the behavioral rhythm respectively. These analyses

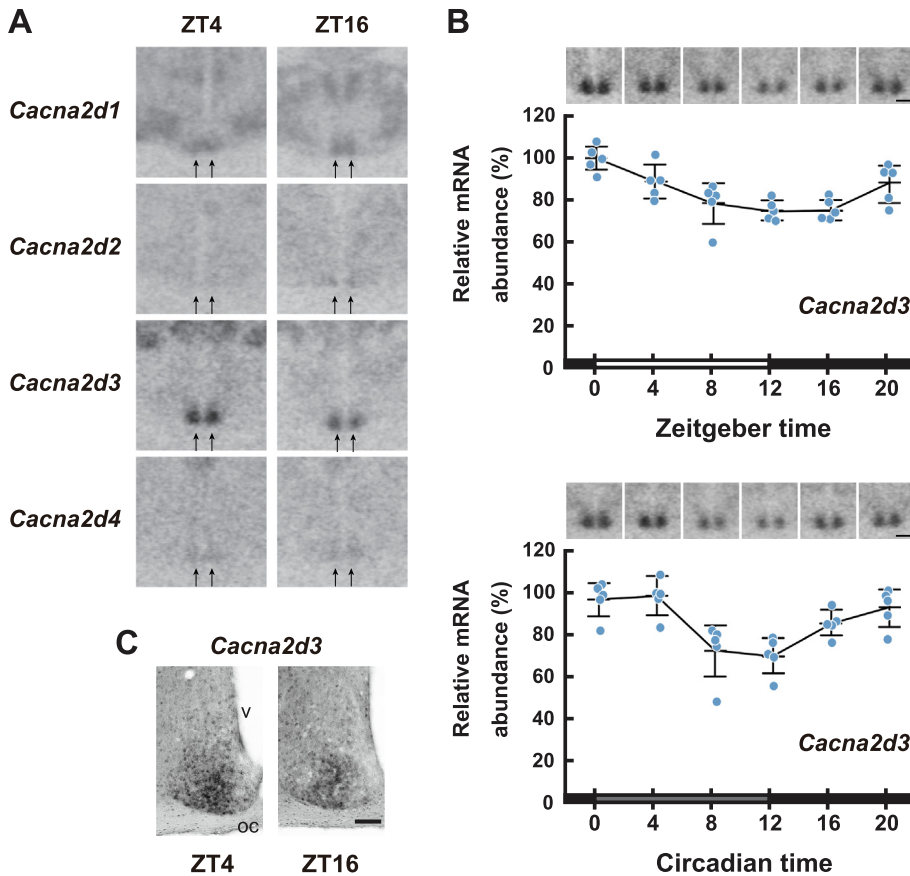


Fig. 1. Circadian expression of the $\alpha 2\delta 3$ subunit of voltage-dependent calcium channels in the SCN. **(A)** Radioisotopic *in situ* hybridization autoradiographs showing the expression of $\alpha 2\delta$ family members in the SCN at Zeitgeber time (ZT)4 and ZT16. Arrows indicate the SCN. Bar, 500 μ m. **(B)** Circadian expression of *Cacna2d3* in the SCN in the light/dark (LD) (top) and constant dark (DD) (bottom) conditions. mRNA abundance was quantified with radioisotopic *in situ* hybridization, and percentage of abundance relative to the highest abundance are presented as means \pm S.E.M. ($n = 5$). Circadian fluctuation of *Cacna2d3* was found both under LD ($p < 0.01$ one-way ANOVA, followed by Sheffe's multiple comparisons; pairwise comparisons showed significant difference $p < 0.01$ between following pairs: ZT0/ZT8, ZT0/ZT12 and ZT0/ZT16) and DD conditions ($p < 0.01$ one-way ANOVA, followed by Sheffe's multiple comparisons; pairwise comparisons showed significant differences $p < 0.05$ between following pairs: CT0/CT8, CT0/CT12, CT4/CT8, CT4/CT12 and CT12/CT20.). Representative autoradiographs at each timepoint are shown on the top (Bar, 200 μ m). **(C)** Digoxigenin *in situ* hybridization showing the distribution of *Cacna2d3*-positive cells in the SCN at ZT4 and ZT16 (OC, optic chiasm; V, third ventricle. Bar, 50 μ m).

revealed virtually identical phase-responses of *Cacna2d3*^{-/-} and WT mice at all timepoints tested (Supplementary Fig. 1). These data indicated that the circadian clock phase-response does not largely depend on $\alpha 2\delta 3$.

Reduced amplitude of circadian locomotor activity rhythm in *Cacna2d3*^{-/-} mice

When actograms of *Cacna2d3*^{-/-} mice were compared with those of WT mice, we noticed a relatively weak amplitude of rhythms in *Cacna2d3*^{-/-} mice in both the LD and DD conditions (Fig. 2B). In brief, we statistically analyzed this phenotypic impression by measuring the rPSD of the dominant 24-h rhythm (0.036–0.048 cycles/h) produced from fast Fourier transform (FFT) analyses of 7 days of animal activity (Siepka and Takahashi, 2005). We found that *Cacna2d3*^{-/-} mice showed a statis-

tically significant reduction in rPSD compared to WT mice in both the LD and DD (Fig. 2D, E) conditions ($*p < 0.05$, $n = 8$, Student's *t*-test, for both LD and DD).

Loss of circadian rhythms of *Cacna2d3*^{-/-} mice in the constant light conditions

It is known that continuous light exposure (LL) elongates the endogenous circadian period length with perturbed rhythm oscillations in the SCN (Steinlechner et al., 2002; Ohta et al., 2005; Doi et al., 2019). We examined the effect of the LL condition on activity rhythm in *Cacna2d3*^{-/-} mice. In accordance with previous reports, periods of locomotor activity rhythms in LL were prolonged in both genotypes (Fig. 3A). We found, however, that there was a difference between WT and *Cacna2d3*^{-/-} mice in the persistence of the rhythms in LL. *Cacna2d3*^{-/-} mice showed a gradual decrease in rhythmicity, with some mice losing stable circadian rhythms in long-lasting LL condition (Fig. 3A; see also Supplementary Fig. 2). rPSD analysis on activity from day 27 in LL revealed a remarkable reduction in circadian amplitude in *Cacna2d3*^{-/-} mice compared to WT mice (Fig. 3B and 3C) ($**p < 0.01$, $n = 8$, Student's *t*-test).

To examine whether the reduced rhythmicity of *Cacna2d3*^{-/-} mice is associated with a defect of clock function in the SCN, we studied *Per1* expression profiles in the SCN in both the DD and LL conditions. *Per1* expression profiles of the mutant mice in DD were indistinguishable from those of WT mice; in both genotypes, circadian *Per1* expression started from the dorsal area at CT0 and spread to the ventral area during CT4–8. Thereafter, *Per1* expression began to decrease, and throughout the subjective night (CT12–20), expression was limited to a few SCN cells (Fig. 3D upper panel). Quantitative *in situ* hybridization analysis of *Per1* expression (Supplementary Fig. 3) also showed no difference between the genotypes throughout the circadian cycle. Another *Period* gene, *Per2*, also did not show genotypic differences of expression rhythm (Supplementary Fig. 4).

On the other hand, when the animals were maintained in LL for 3 weeks, *Per1* expression profiles varied depending on the genotype. In the SCN of WT mice, a clear circadian oscillation of *Per1* with a peak at CT4–8

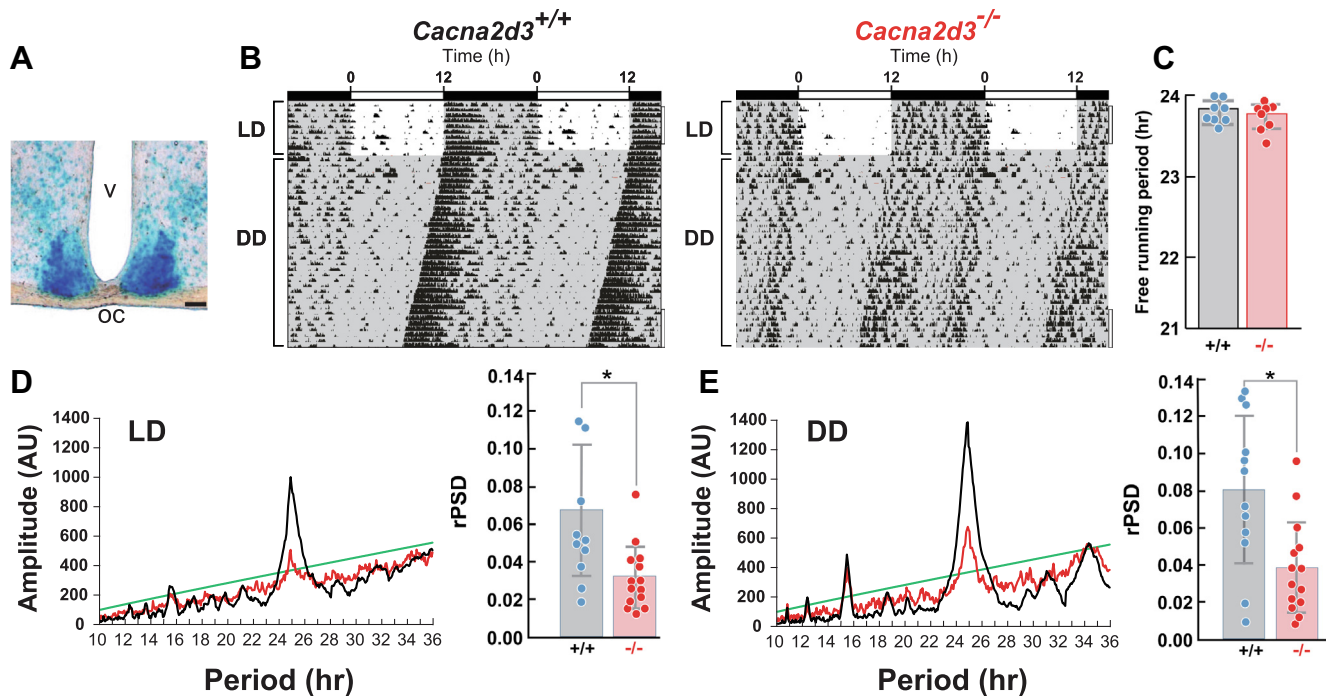


Fig. 2. Attenuated circadian amplitude of locomotor activity in *Cacna2d3*^{-/-} mice. **(A)** β -Gal staining of *Cacna2d3*^{-/-} coronal brain slice (OC, optic chiasm; V, third ventricle. Bar, 100 μ m). **(B)** Representative locomotor activity rhythms of WT (*Cacna2d3*^{+/+}) (left) and *Cacna2d3*^{-/-} (right) mice. Mice initially housed in LD were transferred to DD; dark periods are shown in gray backgrounds. Actograms are shown in double-plotted form. **(C)** Free running periods of WT and *Cacna2d3*^{-/-} mice. Note that the period length between the two genotypes was not significantly different (WT vs *Cacna2d3*^{-/-}; 23.83 \pm 0.05 h vs 23.69 \pm 0.06 h, n = 8 for each genotype). **(D, E)** Representative χ^2 periodograms and rPSD (relative power spectrum distribution; see text for detail) for WT (black) and *Cacna2d3*^{-/-} (red) in LD **(D)** and DD **(E)**. Data were generated from 7-day activity rhythms starting on day 30 in DD as indicated by the black bars in **(B)**. The green line denotes the 0.05 confidence interval. Values of rPSD were reduced in *Cacna2d3*^{-/-} both in LD (WT vs *Cacna2d3*^{-/-}; 0.068 \pm 0.010, n = 12 vs 0.032 \pm 0.005, n = 14; * p < 0.05, Student's t -test) and in DD (WT vs *Cacna2d3*^{-/-}; 0.077 \pm 0.011, n = 12 vs 0.037 \pm 0.006, n = 14; * p < 0.05, Student's t -test).

and a trough at CT16 was observed, although a significant number of *Per1* positive neurons were observed until CT16, even after the peak expression at CT4–8 (Fig. 3D upper panel). In marked contrast, *Cacna2d3*^{-/-} mice failed to exhibit circadian fluctuation of *Per1* expression in the SCN: *Per1* positive neurons were constantly observed throughout the day without clear intra-SCN subdivision specific circadian expression. Namely in LL, a significant number of *Per1* positive neurons were distributed in all of the SCN areas including the ventrolateral part even at CT12 and CT16 in *Cacna2d3*^{-/-} mice (Fig. 3D lower panel). These observations are consistent with the arrhythmic behaviors of the mutant mice.

$\alpha 2\delta 3$ deficiency impairs *Per1* transcription rhythm in organotypic SCN slice cultures

In situ hybridization-based time-course analysis cannot discriminate whether the loss of *Per1* expression rhythms in the SCN is due to a failure of the cell-autonomous clock or a result of a distorted phase organization of properly oscillating cellular clocks. To address this question, we performed real-time bioluminescence imaging of SCN slices prepared from WT and *Cacna2d3*^{-/-} mice carrying a *Per1*-promoter-driven luciferase (*Per1-luc*) transgene, which allows

simultaneous measurement of individual cell oscillations in the SCN (Yamaguchi et al., 2003). In line with *in vivo* data obtained from *Cacna2d3*^{-/-} mice, the luminescence of the *Cacna2d3*^{-/-} SCN slice as a whole showed the clear circadian rhythm with the similar period length as that of the WT slice (WT vs *Cacna2d3*^{-/-}, 24.57 \pm 0.16 h vs 24.45 \pm 0.23 h, n = 3 in both genotypes, p > 0.05, Student's t -test) (Fig. 4A). By the single cell level analysis, however, we noticed that the peak timings of *Per1-luc* luminescence of each neuron were more diversified in *Cacna2d3*^{-/-} SCN cells than WT SCN cells (Fig. 4B). The peak times of the WT vs *Cacna2d3*^{-/-} were significantly different (Kolmogorov–Smirnov, p < 0.0001, n = 750; 250 cells per slice), although the mean period length of each genotype did not differ. Also there was a tendency that cellular peak bioluminescence intensities were decreased in *Cacna2d3*^{-/-} mice. These data indicate that the coherent synchrony was disrupted in *Cacna2d3*^{-/-} mice, and strongly suggest that *Cacna2d3* is required for maintaining synchronized cell oscillations in the SCN.

DISCUSSION

The master clock in the SCN is composed of 16,000 neurons for the paired nucleus (Van den Pol, 1980). Each neuron in the SCN acts as a cell-autonomous molecular

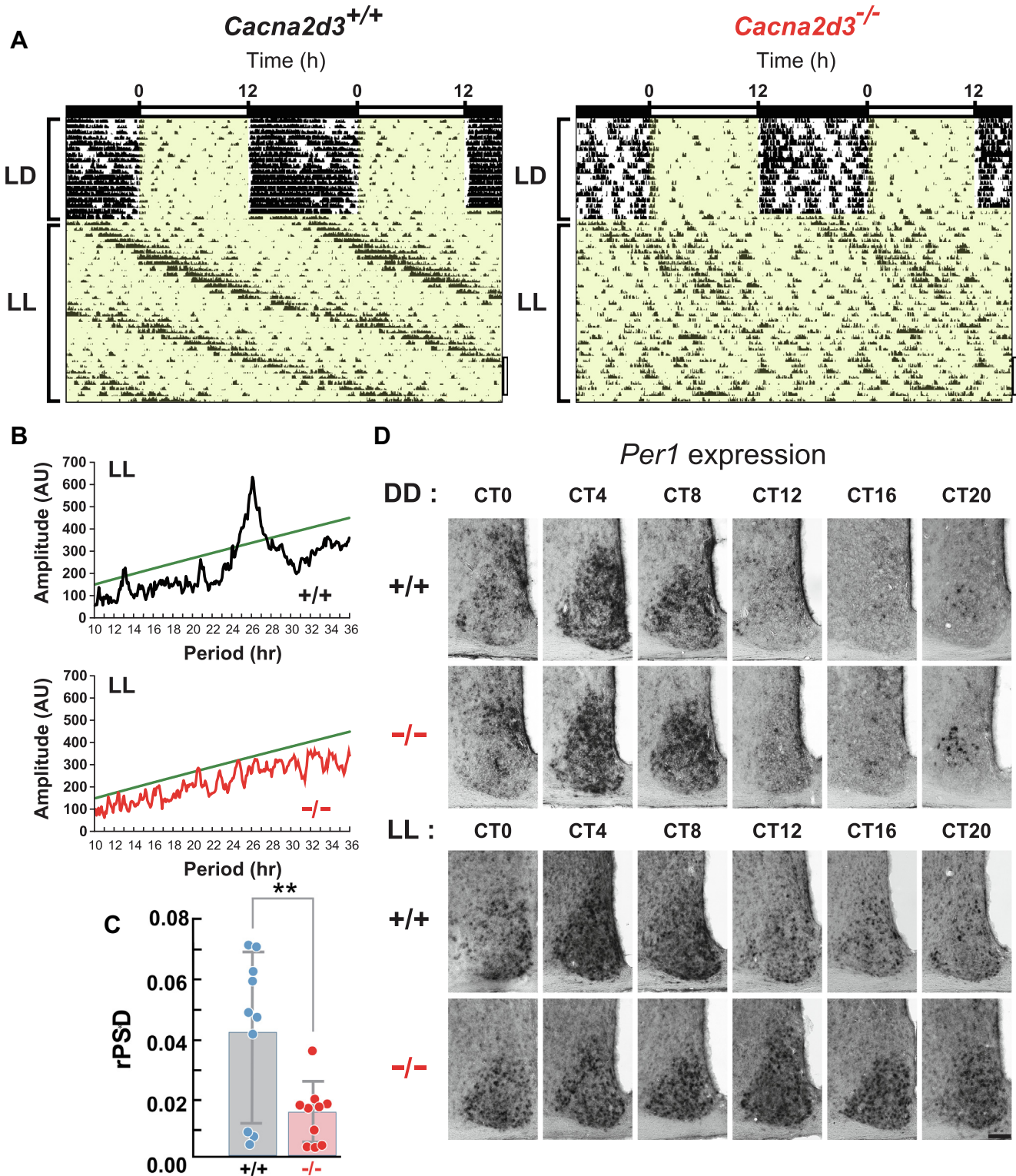


Fig. 3. The constant light (LL) condition dramatically reduced locomotor rhythmicity in *Cacna2d3*^{-/-} mice. **(A)** Representative locomotor activity rhythms of WT (left) and *Cacna2d3*^{-/-} (right) mice. Mice initially housed in LD were transferred to LL. Light terms are indicated by yellow backgrounds. **(B)** Representative χ^2 periodograms for WT (top) and *Cacna2d3*^{-/-} (bottom) mice in LL. Data were generated from 7-day activity rhythms starting on day 27 in LL as indicated by the black bars in **(A)**. The green line denotes the 0.05 confidence interval. **(C)** Circadian amplitude (relative power spectrum distribution, rPSD) for WT (black) and *Cacna2d3*^{-/-} (red) mice in LL. ** $p < 0.01$, Student's *t*-test, $n = 8$ for each genotype. **(D)** Spatiotemporal expression pattern of *Per1* in the SCN of WT and *Cacna2d3*^{-/-} mice either in the DD (top) or the LL condition (bottom). Scale bar, 50 μ m.

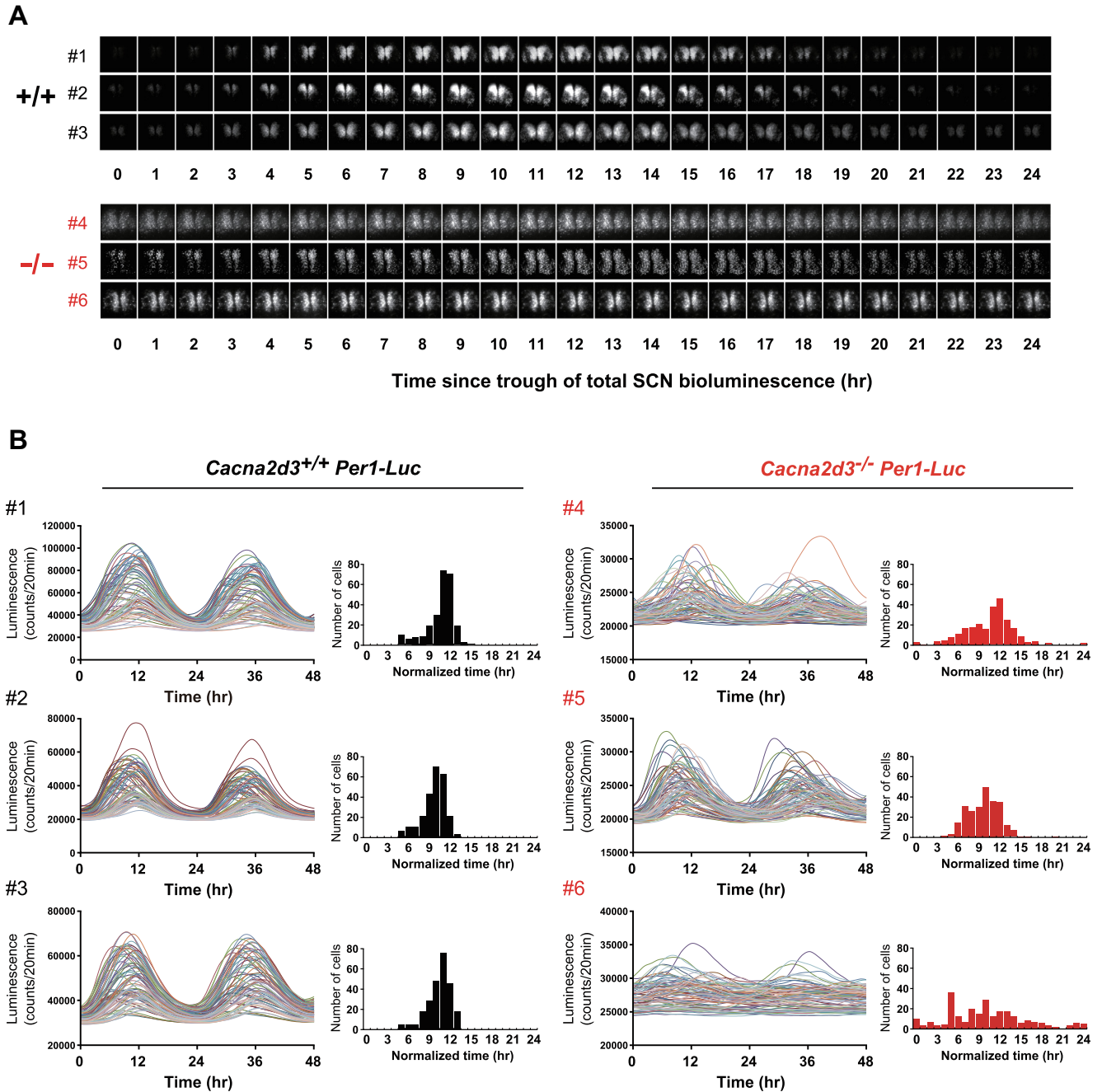


Fig. 4. $\alpha 2\delta 3$ deficiency impairs *Per1* transcription rhythm in organotypic SCN slice cultures. **(A)** Hourly images of the WT (#1–#3) and *Cacna2d3*^{−/−} (#4–#6) SCN slices. Scale bar, 200 μ m. **(B)** Trace of *Per1* transcription fluctuation from single cells (80 cells, on left), and distribution of *Per1* transcription peak time (250 cells, on right). The x axis represents circadian hours (1 h = peak interval/24 h) from the trough time of the total SCN bioluminescence. The first trough time of whole SCN bioluminescence was set to 0. Cells were randomly chosen from three SCN of WT and *Cacna2d3*^{−/−} mice.

oscillator, and the well-coordinated assemblage of these cellular clocks is essential for generating robust oscillation of the circadian rhythms in the SCN (Herzog et al., 2017). The experiment of tetrodotoxin application shows that intercellular synaptic contact in neurons is essential for this synchrony of cellular oscillations (Yamaguchi et al., 2003). Recent studies have shown that the peptidergic signaling is important for synchronization of cellular clock

in the SCN and maintenance of rhythmicity (Maywood et al., 2006; Herzog et al., 2017). By using *Cacna2d3*^{−/−} mice, we demonstrated that a previously uncharacterized membrane-anchored extracellular glycoprotein subtype $\alpha 2\delta 3$ has a role in maintaining the synchrony between SCN neurons and enabling the optimal circadian locomotor activity rhythms to be sustained even under constant light conditions. We first examined the coding gene for

the isoforms of the $\alpha 2\delta$ subunits in the SCN by *in situ* hybridization, and found that *Cacna2d3* is the only isoform highly expressed in the SCN, although *Cacna2d1*, *Cacna2d2*, and *Cacna2d4* are faintly expressed. This suggests that $\alpha 2\delta 3$ is the single isoform which may act in the SCN among the four $\alpha 2\delta$ subtypes.

Like other subtypes, $\alpha 2\delta 3$ is specifically and strongly expressed in the brain (Gong et al., 2001; Cole et al., 2005; Dooley et al., 2007; Hoppa et al., 2012), and is highly concentrated in synaptosomes involved in transmitter release (Hoppa et al., 2012). Interestingly, the *Drosophila* homologue of $\alpha 2\delta 3$, *straightjacket* (CG12295, *stj*) controls the function and development of synapses (Dickman et al., 2008; Ly et al., 2008; Kurshan et al., 2009), suggesting that $\alpha 2\delta 3$ has a role in targeting calcium channels to proper presynaptic sites. In mammals, it is known $\alpha 2\delta 1$ is the neuronal thrombospondin receptor responsible for excitatory brain synaptogenesis (Eroglu et al., 2009). It is recently clarified that $\alpha 2\delta 2$ have synapse-forming ability in cerebellar climbing fiber synapses (Beeson et al., 2020) and in inner hair cell synapses (Fell et al., 2016). All these results point to the likelihood that $\alpha 2\delta 3$ might play some role related to synaptic functions in the brain, but no reports have been clarified yet. Using genome-wide screening of *Drosophila* with heat-nociception, Neely et al. (Neely et al., 2010) identified that $\alpha 2\delta 3$ is evolutionally conserved as a pain gene from fly to mouse/human. In the present study, we examined the role of $\alpha 2\delta 3$ in circadian rhythm generation in the SCN, and found that the impairment of the synchrony of *Per1*-oscillation in the $\alpha 2\delta 3$ knockout mice.

In situ hybridization analysis revealed that *Cacna2d3* is confined to the ventrolateral part of the SCN, in which light evokes molecular events to induce phase-shift of the circadian behavior (Abrahamson and Moore, 2001; Doi et al., 2011). However, we found that the responsiveness to brief light in the *Cacna2d3*-knockout mice was the same as that in WT mice: the magnitude of phase-delay at CT14 and that of phase-advance at CT22 was almost identical to that in WT mice. This finding suggests that the $\alpha 2\delta 3$ may not be involved with the phase-dependent phase-shift of the circadian clock, although it is speculated that VDCC is involved in phase shift in an *ex vivo* analysis (Kim et al., 2005), and in $\alpha 1$ -VDCC-knockout mice (Schmutz et al., 2014). This suggests that $\alpha 2\delta 3$ may act independently of VDCC, or the deletion of $\alpha 2\delta 3$ subunit does not have a major role on VDCC-mediated phase-shift by short exposure of light.

In contrast, continuous exposure to light (LL) elongates the circadian period length with decrease of the amplitude of behavioral rhythms (Daan and Pittendrigh, 1976), although the detailed mechanism involved remains disputed. In SCN slices, it has been reported that LL disrupts the rhythms of the neural firing rate or the rate of glucose utilization (Schwartz and Gainer, 1977; Shibata et al., 1984; Yu et al., 1993). The previous report showed that LL impaired the synchronization of cellular *Per1*-GFP rhythms in the neonatal mice SCN (Steinlechner et al., 2002; Ohta et al., 2005). Here, we found that cellular *Per1* mRNA expression in the SCN with peak at CT4 in the DD or in LD conditions,

became broader in the LL condition: that is, *Per1* expression in LL SCN was observed in some cells even at CT12, CT16, and CT20, when no cells were observed in the LD/DD conditions. The inhibitory effect of LL condition on behavioral rhythm was more remarkable in $\alpha 2\delta 3$ -knockout mice: The gene ablation of $\alpha 2\delta 3$ led to reduction in locomotor amplitude to an arrhythmic level in the LL condition. We also detected that the spatiotemporal circadian expression of *Per1* mRNA in the SCN *in vivo* was abolished in $\alpha 2\delta 3$ -knockout mice in the LL condition. These strongly suggests that prolonged light exposure perturbs the original synchronization of cellular oscillations in the SCN master clock when it is deficient in synapse-rich $\alpha 2\delta 3$. Because communication between neurons is essential for sustained daily oscillations of the SCN (Yamaguchi et al., 2003), the vulnerable locomotor rhythm of *Cacna2d3*^{-/-} mice in LL may be the result of a weaker output signal from the SCN due to the desynchronization of cellular clocks caused by continuous light stimulations.

We further examined cellular oscillations in organotypic SCN cultures of $\alpha 2\delta 3$ -knockout mice bearing *Per1-luc*. Relative to the dorsomedial-ventrolateral spatiotemporal expression pattern of WT SCN, we found that the cellular rhythms within each SCN slice jolted out of alignment in *Cacna2d3*^{-/-} mice. Lower amplitude of each cellular peaks was also noted in *Cacna2d3*^{-/-} slices, although the methodological limitation of slice culture system should be taken into consideration (Yamaguchi et al., 2003; Tominaga-Yoshino et al., 2007). Flattering the peak-trough rhythms with diverged peak timing strongly suggest that *Cacna2d3* is required for maintaining synchronized cell oscillations in the SCN in cultured conditions.

SCN neurons are mostly electrically silent during the night, start to fire action potentials near dawn and then continue to generate action potentials with a slow and steady pace during the day time (Colwell, 2011). As the applications of tetrodotoxin (Yamaguchi et al., 2003) or pertussis toxin (Aton et al., 2006; Doi et al., 2011) dampened rhythms of SCN neurons, intercellular communications are indispensable for generating daily rhythm of the SCN through controlling transcriptional and translational feedback loop of clock genes. Since it is already demonstrated that various VDCC subunits including L-type, P/Q-type and T-type have also been expressed in the SCN (Pennartz et al., 2002; Cloues and Sather, 2003; Kim et al., 2005; Nahm et al., 2005), further study using calcium imaging or synaptic staining would better address the role of VDCCs including $\alpha 2\delta 3$ in circadian rhythm formation.

In conclusion, we provided evidence that the $\alpha 2\delta 3$ contributes to form the synchronization of cellular rhythms among SCN neurons to generate robust rhythms. $\alpha 2\delta 3$ deficiency does not disrupt cellular oscillations, but the strength of circadian oscillation as a whole SCN is decreased. Taking into account the role of $\alpha 2\delta 3$ in synapse formation, synaptic connection, spine maturation important for neurotransmission in presynaptic terminals (Dolphin, 2012; Ablinger et al., 2020), it can be predicted that synchronization among

SCN clock neurons were impaired in *Cacna2d3*-knockout mice.

ADDITIONAL INFORMATION

The author(s) declare no additional interests.

AUTHOR CONTRIBUTIONS

Author contributions: M.M. and H.O. designed the research; M.M. and K.S. contributed equally as first authors who performed experiments in collaboration with N.M, F.Y., S.U., N.Y., M.D., K.T. and H.O., and H.O., M.M. and K.S. drafted the manuscript.

ACKNOWLEDGEMENTS

This work was supported by the Core Research for Evolutional Science and Technology, Japan Science and Technology Agency (JPMJCR14W3), and the Ministry of Education, Culture, Sports, Science and Technology of Japan (15H01843, 18H04015, 17K01986, 18H02606), and SRF.

REFERENCES

- Ablinger C, Geisler SM, Stanika RI, Klein CT, Obermair GJ (2020) Neuronal $\alpha(2)\delta$ proteins and brain disorders. *Pflugers Arch* 472:845–863.
- Abrahamson EE, Moore RY (2001) Suprachiasmatic nucleus in the mouse: retinal innervation, intrinsic organization and efferent projections. *Brain Res* 916:172–191.
- Alles SRA, Cain SM, Snutch TP (2020) Pregabalin as a pain therapeutic: beyond calcium channels. *Front Cell Neurosci* 14:83.
- Aton SJ, Huettner JE, Straume M, Herzog E (2006) GABA and Gi/o differentially control circadian rhythms and synchrony in clock neurons. *Proc Natl Acad Sci USA* 103:19188–19193.
- Beeson KA, Beeson R, Westbrook GL, Schnell E (2020) $\alpha 2\delta$ -2 protein controls structure and function at the cerebellar climbing fiber synapse. *J Neurosci* 40:2403–2415.
- Campiglio M, Flucher BE (2015) The role of auxiliary subunits for the functional diversity of voltage-gated calcium channels. *J Cell Physiol* 230:2019–2031.
- Cole RL, Lechner SM, Williams ME, Prodanovich P, Bleicher L, Varney MA, Gu G (2005) Differential distribution of voltage-gated calcium channel alpha-2 delta (alpha2delta) subunit mRNA-containing cells in the rat central nervous system and the dorsal root ganglia. *J Comp Neurol* 491:246–269.
- Cloues RK, Sather WA (2003) Afterhyperpolarization regulates firing rate in neurons of the suprachiasmatic nucleus. *J Neurosci* 23:1593–1604.
- Colwell CS (2011) Linking neural activity and molecular oscillations in the SCN. *Nat Rev Neurosci* 12:553–569.
- Daan S, Pittendrigh CS (1976) A Functional analysis of circadian pacemakers in nocturnal rodents. III. Heavy water and constant light: homeostasis of frequency?. *J Comp Physiol A* 106:267–290.
- Dickman DK, Kurshan PT, Schwarz TL (2008) Mutations in a *Drosophila* alpha2delta voltage-gated calcium channel subunit reveal a crucial synaptic function. *J Neurosci* 28:31–38.
- Doi M, Ishida A, Miyake A, Sato M, Komatsu R, Yamazaki F, Kimura I, Tsuchiya S, et al. (2011) Circadian regulation of intracellular G-protein signalling mediates intercellular synchrony and rhythmicity in the suprachiasmatic nucleus. *Nat Commun* 2:327.
- Doi M, Shimatani H, Atobe Y, Murai I, Hayashi H, Takahashi Y, Fustin JM, Yamaguchi Y, et al. (2019) Non-coding cis-element of *Period2* is essential for maintaining organismal circadian behaviour and body temperature rhythmicity. *Nat Commun* 10:2563.
- Dolphin AC (2012) Calcium channel auxiliary $\alpha 2\delta$ and β subunits: trafficking and one step beyond. *Nat Rev Neurosci* 13:542–555.
- Dooley DJ, Taylor CP, Donevan S, Feltner D (2007) Ca²⁺ channel alpha2delta ligands: novel modulators of neurotransmission. *Trends Pharmacol Sci* 28:75–82.
- Dworkin RH, O'Connor AB, Backonja M, Farrar JT, Finnerup NB, Jensen TS, Kalso EA, Loeser JD, et al. (2007) Pharmacologic management of neuropathic pain: evidence-based recommendations. *Pain* 132:237–251.
- Eroglu C, Allen NJ, Susman MW, O'Rourke NA, Park CY, Ozkan E, Chakraborty C, Mulinyawe SB, et al. (2009) Gabapentin receptor alpha2delta-1 is a neuronal thrombospondin receptor responsible for excitatory CNS synaptogenesis. *Cell* 139:380–392.
- Fell B, Eckrich S, Blum K, Eckrich T, Hecker D, Obermair GJ, Münkner S, Flockerzi V, et al. (2016) $\alpha 2\delta 2$ Controls the function and trans-synaptic coupling of Cav1.3 channels in mouse inner hair cells and is essential for normal hearing. *J Neurosci* 36:11024–11036.
- Field MJ, Cox PJ, Stott E, Melrose H, Offord J, Su TZ, Bramwell S, Corradini L, et al. (2006) Identification of the alpha2-delta-1 subunit of voltage-dependent calcium channels as a molecular target for pain mediating the analgesic actions of pregabalin. *Proc Natl Acad Sci U S A* 103:17537–17542.
- Gong HC, Hang J, Kohler W, Li L, Su TZ (2001) Tissue-specific expression and gabapentin-binding properties of calcium channel alpha2delta subunit subtypes. *J Membr Biol* 184:35–43.
- Harrisingh MC, Nitabach MN (2008) Circadian rhythms. Integrating circadian timekeeping with cellular physiology. *Science* 320:879–880.
- Herzog ED, Hermansteyne T, Smyllie NJ, Hastings MH (2017) Regulating the suprachiasmatic nucleus (SCN) circadian clockwork: interplay between cell-autonomous and circuit-level mechanisms. *Cold Spring Harb Perspect Biol* 9.
- Hoppa MB, Lana B, Margas W, Dolphin AC, Ryan TA (2012) $\alpha 2\delta$ expression sets presynaptic calcium channel abundance and release probability. *Nature* 486:122–125.
- Iftikhar IH, Alghothani L, Trotti LM (2017) Gabapentin enacarbil, pregabalin and rotigotine are equally effective in restless legs syndrome: a comparative meta-analysis. *Eur J Neurol* 24:1446–1456.
- Kim DY, Choi HJ, Kim JS, Kim YS, Jeong DU, Shin HC, Kim MJ, Han HC, et al. (2005) Voltage-gated calcium channels play crucial roles in the glutamate-induced phase shifts of the rat suprachiasmatic circadian clock. *Eur J Neurosci* 21:1215–1222.
- Kurshan PT, Oztan A, Schwarz TL (2009) Presynaptic alpha2delta-3 is required for synaptic morphogenesis independent of its Ca²⁺-channel functions. *Nat Neurosci* 12:1415–1423.
- Ly CV, Yao CK, Verstreken P, Ohyama T, Bellen HJ (2008) straightjacket is required for the synaptic stabilization of cacophony, a voltage-gated calcium channel alpha1 subunit. *J Cell Biol* 181:157–170.
- Maywood ES, Reddy AB, Wong GK, O'Neill JS, O'Brien JA, McMahon DG, Harmar AJ, Okamura H, et al. (2006) Synchronization and maintenance of timekeeping in suprachiasmatic circadian clock cells by neuropeptidergic signaling. *Curr Biol* 16:599–605.
- Mohawk JA, Green CB, Takahashi JS (2012) Central and peripheral circadian clocks in mammals. *Annu Rev Neurosci* 35:445–462.
- Nahm SS, Farnell YZ, Griffith W, Earnest DJ (2005) Circadian regulation and function of voltage-dependent calcium channels in the suprachiasmatic nucleus. *J Neurosci* 25:9304–9308.
- Neely GG, Hess A, Costigan M, Keene AC, Goulas S, Langeslag M, Griffin RS, Belfer I, et al. (2010) A genome-wide *Drosophila* screen for heat nociception identifies $\alpha 2\delta 3$ as an evolutionarily conserved pain gene. *Cell* 143:628–638.
- Nitabach MN, Blau J, Holmes TC (2002) Electrical silencing of *Drosophila* pacemaker neurons stops the free-running circadian clock. *Cell* 109:485–495.

- Ohta H, Yamazaki S, McMahon DG (2005) Constant light desynchronizes mammalian clock neurons. *Nat Neurosci* 8:267–269.
- Okamura H (2007) Suprachiasmatic nucleus clock time in the mammalian circadian system. *Cold Spring Harb Symp Quant Biol* 72:551–556.
- Pennartz CM, de Jeu MT, Bos NP, Schaap J, Geurtsen AM (2002) Diurnal modulation of pacemaker potentials and calcium current in the mammalian circadian clock. *Nature* 416:286–290.
- Reppert SM, Weaver DR (2002) Coordination of circadian timing in mammals. *Nature* 418:935–941.
- Schmutz I, Chavan R, Ripperger JA, Maywood ES, Langwieser N, Jurik A, Stauffer A, Delorme JE, et al. (2014) A specific role for the REV-ERB α -controlled L-Type Voltage-Gated Calcium Channel CaV1.2 in resetting the circadian clock in the late night. *J Biol Rhythms* 29:288–298.
- Schwartz WJ, Gainer H (1977) Suprachiasmatic nucleus: use of ¹⁴C-labeled deoxyglucose uptake as a functional marker. *Science* 197:1089–1091.
- Shibata S, Liou S, Ueki S, Oomura Y (1984) Influence of environmental light-dark cycle and enucleation on activity of suprachiasmatic neurons in slice preparations. *Brain Res* 302:75–81.
- Shigeyoshi Y, Taguchi K, Yamamoto S, Takekida S, Yan L, Tei H, Moriya T, Shibata S, Loros JJ, Dunlap JC, Okamura H (1997) Light-induced resetting of a mammalian circadian clock is associated with rapid induction of the mPer1 transcript. *Cell* 91:1043–1053.
- Siepkha SM, Takahashi JS (2005) Methods to record circadian rhythm wheel running activity in mice. *Methods Enzymol* 393:230–239.
- Steinlechner S, Jacobmeier B, Scherbarth F, Dernbach H, Kruse F, Albrecht U (2002) Robust circadian rhythmicity of Per1 and Per2 mutant mice in constant light, and dynamics of Per1 and Per2 gene expression under long and short photoperiods. *J Biol Rhythms* 17:202–209.
- Tominaga-Yoshino K, Ueyama T, Okamura H: Suprachiasmatic nucleus cultures that maintain rhythmic properties in vitro. In *Methods in Molecular Biology*, vol. 362: *Circadian Rhythms: Methods and Protocols*, Edited by E. Rosato, Humana Press Inc., Totowa, NJ, 2007, pp481–492.
- Van den Pol AN (1980) The hypothalamic suprachiasmatic nucleus of rat: intrinsic anatomy. *J Comp Neurol* 191:661–702.
- Winkelman JW, Armstrong MJ, Allen RP, Chaudhuri KR, Ondo W, Trenkwalder C, Zee PC, Gronseth GS, et al. (2016) Practice guideline summary: treatment of restless legs syndrome in adults: Report of the Guideline Development, Dissemination, and Implementation Subcommittee of the American Academy of Neurology. *Neurology* 87:2585–2593.
- Yamaguchi S, Isejima H, Matsuo T, Okura R, Yagita K, Kobayashi M, Okamura H (2003) Synchronization of cellular clocks in the suprachiasmatic nucleus. *Science* 302:1408–1412.
- Yamaguchi S, Mitsui S, Miyake S, Yan L, Onishi H, Yagita K, Suzuki M, Shibata S, et al. (2000) The 5' upstream region of mPer1 gene contains two promoters and is responsible for circadian oscillation. *Curr Biol* 10:873–876.
- Yu GD, Rusak B, Piggins HD (1993) Regulation of melatonin-sensitivity and firing-rate rhythms of hamster suprachiasmatic nucleus neurons: constant light effects. *Brain Res* 602:191–199.

APPENDIX A. SUPPLEMENTARY DATA

Supplementary data to this article can be found online at <https://doi.org/10.1016/j.neuroscience.2021.02.016>.

(Received 7 October 2020, Accepted 10 February 2021)
(Available online 18 February 2021)